Copyright © 2010 Tech Science Press MCB, vol.7, no.4, pp.213-224, 2010

Dynamic Effects on the Formation and Rupture of Aneurysms

J.S. Ren*

Abstract: Dynamic analysis of an axially stretched arterial wall with collagen fibers distributed in two preferred directions under a suddenly applied constant internal pressure along with the possibility of the formation and rupture of aneurysm are examined within the framework of nonlinear dynamics. A two layer tube model with the fiber-reinforced composite-based incompressible anisotropic hyper-elastic material is employed to model the mechanical behavior of the arterial wall. The maximum amplitudes and the phase diagrams are given by numerical computation of the differential relation. It is shown that the arterial wall undergoes nonlinear periodic oscillation and no aneurysms are formed under the normal condition. However, an aneurysm may be formed under such abnormal conditions as the stiffness of the fibers is deduced or the direction of the fibers is oriented towards the axial direction. Furthermore, the possibility for the rupture of aneurysm is discussed with the distribution of stresses.

Keywords: arterial wall with collagen fibers, aneurysm, incompressible anisotropic hyper-elastic material, nonlinear periodic oscillation, formation and rupture

1 Introduction

In recent years, more and more people in the world are suffering from aneurysms (Humphrey2002, Humphrey2003b). Beginning as a small dilatation of the arterial wall, aneurysms may expand to over 10 cm in diameter along with rapidly expanding as shown in Fig.1 (Watton et. al.2004). Finally, aneurysms might rupture in some cases for a rate of 24.9 % and this will give rise to devastating consequences for a rate of 90 % (He et al 1993, Lanne et al. 1992, Papahariluon et al. 2006, Volokh and Vorp2008). Parts of the patients die whereas many of the survivors suffer severe functional deficits. It continues to be one of the main causes of significant morbidity and mortality. At the same time, current aneurysm treatment is expensive and carries considerable morbidity and mortality risks (Vorp2007).

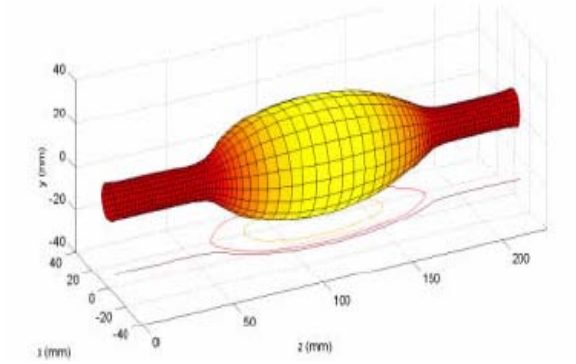

Figure 1: Schematic representation of an aneurysm (modified from Watton et al. 2003)

Clearly, there is a need to combine geometrical, mechanical and histological methods to understand the mechanism of aneurysms (Humphrey2003b, Watton et. al. 2004, Wilmink et al. 1995). It is also helpful for the development of soft tissue biomechanics and tissue engineering (Neren and Selihtar 2001). There are some theories with regard to the formation or pathogenesis of aneurysms but little general agreement (Humphrey2002, Humphrey2003a, David and Humphrey2003, Volokh and Vorp2008, Vorp2007). With regard to the rupture of aneurysms, it is widely thought that the rupture occurs when the wall stress of the aneurysm ex-

* Department of Mechanics, Shanghai institute of applied Mathematics and Mechanics, Shanghai University, Shanghai 200444, China

ceeds its wall strength following basic principles of material failure (Humphrey2003b, Volokh and Vorp2008, Vorp2007). So it is vital to understand well the mechanism of aneurysm wall (Kroon2008). However, the mechanical behavior of arterial wall is complex and highly nonlinear in general as they often involve three-dimensional geometry, dynamic loading conditions and fluid-solid interaction (Olsenl et. al. 1999, Holzapfel et. al.2002, Humphrey2002).

From the point of histological view, arterial wall is a layered structure composed of three layers: intima, media, adventitia (Holzapfel et al. 2004). The contribution of the intima to the mechanical properties of the arterial wall is negligible. In the media and adventitia, collagen fibers are arranged in helically distributed families which induce the anisotropy in the mechanical response of the arterial wall as shown in Fig.2 (Holzapfel et. al.1998, Holzapfel et al. 2000, Driessen et. al.2003, Humphrey 2002, Driessen et. al.2004).

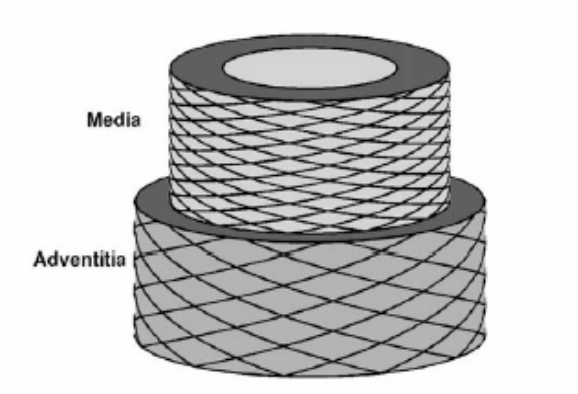

Figure 2: Schematic representation of typical fiber architecture in an arterial wall (Holzapfel et al. 2000, with a modification by Driessen et al. 2004)

Pseudo-elasticity allows the use of nonlinear elasticity theory to study as a first approximation for many types of soft tissues (Fung1990). In practice, most researches, more commonly, simply assume that the material is elastic with constitutive relation based only on loading curves. This approach has provided useful approximate results in a large number of problems (Ogden2002). Following Fung, most pseudo-elastic constitutive models for the arterial wall are build in the form of exponential and logarithmic strain energy density functions (Vito and Dixon2003). While some of the newest constitutive models are built incorporating the histology-derived micro-structure (Holzapfel et. al. 2000, Ogden2003).

Till now, much of the literature on such mechanics deals with elasto-statics and they have been extensively studied (Holzapfel and Ogden2003, Ren2007). The mechanical behavior of soft tissue under quasi-static loading is dominated by the performance of its fibrous components, primarily collagen and elastin fibers. However, many physical problems are inherently dynamic, so the analysis of elasto-dynamics is important (David and Humphrey2003, Holzapfel et. al.2002, Humphrey2002). As an example, intracranial aneurysms are typically subject to periodic or nearly periodic internal pressures (Humphrey1998, Haslach and Humphrey2004). The system is autonomous when the forcing internal pressure is constant (Chou-wang and Horgan 1989).

The purpose of the present paper is to investigate the dynamic effect on the possibility of the formation and rupture of aneurysm within the framework of nonlinear elasto-dynamics. Based on the fiber-reinforced composite material model developed by Holzapfel et. al. (Holzapfel et. al. 2000) and view the arterial wall as a two layer thin-walled tube, the dynamic response of the arterial wall with collagen fibers distributed in two preferred directions under a suddenly applied constant internal pressure is investigated. An exact differential relation between the deformation of the arterial wall and the applied pressure is obtained at first. The maximum amplitudes and the phase diagrams are given by numerical computation. It is shown that the arterial wall undergoes nonlinear periodic oscillation and no aneurysms are formed under the normal condition through dynamic analyzes as usual. However, an aneurysm may be formed in arterial walls under such abnormal conditions as the stiffness of the fibers is decreased or the direction of the fibers is oriented towards the axial direction.

Through numerical computation of the distribution of stresses of the aneurysm, it is proved that the rupture of aneurysm is doomed as the stress under the normal blood pressure is larger than the critical breaking stress of the aneurysm. It is hoped that this paper will increase our understanding of the mechanics of aneurysm, including its three phases: pathogenesis, enlargement, and rupture.

2 Strain energy function

As shown in Fig.2, the collagen fibers of the arterial wall are arranged in two helically distributed families with a small pitch and very little dispersion in their orientation. Based on the study of Holzapfel et al. (Holzapfel et al. 2000), the arterial wall is modeled as an incompressible fiber-reinforced composite material, in which the collagen fibers are viewed as a one-dimensional material which exerting only stress in the fiber direction. With the assumption of the incompressible matrix and fiber, the strain energy function for the arterial wall derived from hyper-elasticity can be expressed as

$$W = W_M + W_F \tag{1}$$

In which, W_M is the strain energy function for the matrix (Haugton et. al. 1978)

$$W_M = \sum_r \frac{\mu_r}{\alpha_i}\left(\lambda_r^{\alpha_r} + \lambda_\theta^{\alpha_r} + \lambda_z^{\alpha_r} - 3\right) \tag{2}$$

with constants: $\alpha_1 = 1.3, \alpha_2 = 5.0, \alpha_3 = -2.0, \mu_1 = 1.491\mu, \mu_2 = 0.003\mu, \mu_3 = -0.023\mu, \mu$ is the shear modulus for the arterial wall, $\lambda_r, \lambda_\theta, \lambda_z$ are the principal stretches. W_F is the strain energy function for the collagen fiber (Driessen et. al.2004)

$$W_F = \frac{k_1}{2k_2} e^{k_2\left(\lambda^2-1\right)^2} \tag{3}$$

In which, λ is the fiber stretch. Constant k_1 is the stiffness of the collagen fiber and k_2 describes the degree of its nonlinearity. The corresponding Cauchy stress may be written as

$$\sigma = -p(r,t)\mathbf{I} + \tau(\mathbf{B}) + \sum_{j=1}^{2} \psi_f^j\left(\lambda_j^2\right)\mathbf{e}_f^j\mathbf{e}_f^j \tag{4}$$

Where, $p(r,t)$ is the hydrostatic pressure to be determined, $\mathbf{I}$ is the unit tensor, τ is the isotropic matrix stress, $\psi_f = 2k_1\lambda^2\left(\lambda^2-1\right)e^{k_2\left(\lambda^2-1\right)^2}$ is the fiber stress, $\mathbf{B} = \mathbf{F}\cdot\mathbf{F}^T$ is the left Cauchy-Green deformation tensor, $\mathbf{F}$ is the deformation-gradient tensor, $\mathbf{e}_f$ is the fiber direction in the deformed configuration.

The fiber stretch may be calculated from

$$\lambda = \sqrt{\mathbf{e}_{f0}\cdot\mathbf{C}\cdot\mathbf{e}_{f0}} \tag{5}$$

Where, $\mathbf{e}_{f0}$ is the fiber direction in the undeformed configuration and $\mathbf{C} = \mathbf{F}^T\cdot\mathbf{F}$ is the right Cauchy-Green deformation tensor. The fiber direction in the deformed configuration is determined from that in the undeformed configuration by

$$\lambda\mathbf{e}_f = \mathbf{F}\mathbf{e}_{f0} \tag{6}$$

3 Formulations

An axially stretched arterial wall subjected to a constant internal pressure suddenly applied may be considered as the dynamical response of a two layer tube with inner radius A and outer radius$B$. The media and the adventitia of the arterial wall are conglutinated at the interface with radius$D\,(A<D<B)$. Assume that the undeformed and deformed configurations are described by the cylindrical coordinate systems (R,Θ,Z) and(r,θ,z), respectively. The motion of the tube is

$$r = r(R,t) > 0, A \le R \le B,\ \theta = \Theta,\ z = \lambda_z Z \tag{7}$$

Where, $r(R,t)$ is a function to be determined, λ_z is the axial stretch of the tube.

The corresponding deformation-gradient tensor $\mathbf{F}$ is

$$\mathbf{F} = \mathrm{diag}\left(\dot{r}(R,t), r(R,t)/R, \lambda_z\right) = \mathrm{diag}\left(\lambda_r, \lambda_\theta, \lambda_z\right), \tag{8}$$

The principal stretches are

$$\lambda_r = \dot{r}(R,t), \quad \lambda_\theta = r(R,t)/R,\ \lambda_z = \lambda_z \tag{9}$$

The corresponding right or left Cauchy-Green deformation tensor is

$$\mathbf{C}=\mathbf{B}=\operatorname{diag}\left(\dot{r}^2(R,t),r^2(R,t)/R^2,\lambda_z^2\right) \tag{10}$$

The motion equations for the tube in the absence of body forces are

$$\frac{\mathrm{d}\sigma_{rr}^m}{\mathrm{d}r}+\frac{1}{r}\left[\sigma_{rr}^m-\sigma_{\theta\theta}^m\right]=\rho\ddot{r} \tag{11a}$$

$$\frac{\mathrm{d}\sigma_{rr}^a}{\mathrm{d}r}+\frac{1}{r}\left[\sigma_{rr}^a-\sigma_{\theta\theta}^a\right]=\rho\ddot{r} \tag{11b}$$

Where, ρ is the density of the material. $\sigma_{rr}^m,\sigma_{\theta\theta}^m,\sigma_{zz}^m$ represent stress components of the media, and $\sigma_{rr}^a,\sigma_{\theta\theta}^a,\sigma_{zz}^a$ represent stress components of the adventitia given by Eq. (4), respectively. Without special announcement in this paper, the superscript m denotes the media part for $A\le R\le D$ and the superscript a denotes the adventitia part for $D\le R\le B$. The boundary conditions are

$$\begin{aligned}&\sigma_{rr}^m(a,t)=-p_0,\quad t\ge 0\\&\sigma_{rr}^a(b,t)=0,\quad t\ge 0\end{aligned} \tag{12}$$

Where, p_0 is the constant internal pressure suddenly applied on the inner surface. $a=r(A,t)$ and $b=r(B,t)$ are the deformed inner and outer surface, respectively.

From continuity of the radial stress σ_{rr} at the interface of the media and the adventitia

$$\sigma_{rr}^m(r,t)=\sigma_{rr}^a(r,t),r=d \tag{13}$$

Where, $d=r(D,t)$. The initial conditions for the arterial wall are

$$\begin{aligned}&r(R,0)=R\\&\dot{r}(R,0)=0\end{aligned} \tag{14}$$

4 Solutions

The incompressibility condition of the material may be expressed as

$$r^2-a^2=\frac{1}{\lambda_z}\left(R^2-A^2\right) \tag{15}$$

Letting

$$v=v(r)=\frac{r}{R}=\left(\lambda_z\left(1-\frac{a^2}{r^2}\right)+\frac{A^2}{r^2}\right)^{-\frac{1}{2}} \tag{16}$$

Then,

$$\lambda_\theta=v,\lambda_r=\lambda_z^{-1}v^{-1} \tag{17}$$

Assume that the collagen fibers align with preferred directions $\mathbf{e}_{f0}^i$, directed among the axial direction with angle β. Then the directions for two families of collagen fibers may be written as

$$\mathbf{e}_{f0}^1=\begin{Bmatrix}0\\\sin\beta\\\cos\beta\end{Bmatrix},\quad \mathbf{e}_{f0}^2=\begin{Bmatrix}0\\-\sin\beta\\\cos\beta\end{Bmatrix} \tag{18}$$

Then, from Eq. (5), (10) and (18),

$$\lambda_1=\lambda_2=\lambda=\sqrt{\sin^2\beta v^2+\cos^2\beta\lambda_z^2} \tag{19}$$

From Eq. (6), (18) and (19), we have

$$\mathbf{e}_f^1=\frac{1}{\lambda}\begin{Bmatrix}0\\\sin\beta v\\\cos\beta\lambda_z\end{Bmatrix},\quad \mathbf{e}_f^2=\frac{1}{\lambda}\begin{Bmatrix}0\\-\sin\beta v\\\cos\beta\lambda_z\end{Bmatrix} \tag{20}$$

Here, the direction of collagen fibers β for the media and adventitia may take different values β_m and β_a in Eq. (18), (19) and (20). Then, from Eq. (4), non-zero stresses for the media and adventitia are

$$\begin{aligned}\sigma_{rr}^m(r,t)&=-p^m(r,t)+\sum_r\mu_{\alpha_r}^m\lambda_z^{-\alpha_r}v^{-\alpha_r}\\\sigma_{\theta\theta}^m(r,t)&=-p^m(r,t)+\sum_r\mu_{\alpha_r}^m v^{\alpha_r}\\&\quad+4k_1^m\left(\lambda_m^2-1\right)e^{k_2^m\left(\lambda_m^2-1\right)^2}\sin^2\beta_m v^2\\\sigma_{zz}^m(r)&=-p^m(r,t)+\sum_r\mu_{\alpha_r}^m\lambda_z^{\alpha_r}\\&\quad+4k_1^m\left(\lambda_m^2-1\right)e^{k_2^m\left(\lambda_m^2-1\right)^2}\cos^2\beta_m\lambda_z^2\end{aligned} \tag{21a}$$

$$\begin{aligned}\sigma_{rr}^a(r,t)&=-p^a(r,t)+\sum_r\mu_{\alpha_r}^a\lambda_z^{-\alpha_r}v^{-\alpha_r}\\\sigma_{\theta\theta}^a(r)&=-p^a(r,t)+\sum_r\mu_{\alpha_r}^a v^{\alpha_r}\\&\quad+4k_1^a\left(\lambda_a^2-1\right)e^{k_2^a\left(\lambda_a^2-1\right)^2}\sin^2\beta_a v^2\\\sigma_{zz}^a(r)&=-p^a(r,t)+\sum_r\mu_{\alpha_r}^a\lambda_z^{\alpha_r}\\&\quad+4k_1^a\left(\lambda_a^2-1\right)e^{k_2^a\left(\lambda_a^2-1\right)^2}\cos^2\beta_a\lambda_z^2\end{aligned}$$

(21b)

Differentiating Eq. (15) with respect to t,

$$\ddot{r}(R,t)=\frac{1}{r}[(1-\frac{a^2}{r^2})\dot{a}^2+a\ddot{a}] \tag{22}$$

$$\sigma^m_{rr}(r)=-p^m(r)+\sum_r \mu^m_{\alpha_r}\lambda_z^{-\alpha_r}v^{-\alpha_r}$$

$$\sigma^m_{\theta\theta}(r)=-p^m(r)+\sum_r \mu^m_{\alpha_r}v^{\alpha_r}$$
$$+4k^m_1\left(\lambda^2_m-1\right)e^{k^m_2\left(\lambda^2_m-1\right)^2}\sin^2\beta_m v^2$$

$$\sigma^m_{zz}(r)=-p^m(r)+\sum_r \mu^m_{\alpha_r}\lambda_z^{\alpha_r}$$
$$+4k^m_1\left(\lambda^2_m-1\right)e^{k^m_2\left(\lambda^2_m-1\right)^2}\cos^2\beta_m\lambda_z^2$$

$$\sigma^a_{rr}(r)=-p^a(r)+\sum_r \mu^a_{\alpha_r}\lambda_z^{-\alpha_r}v^{-\alpha_r}$$

$$\sigma^a_{\theta\theta}(r)=-p^a(r)+\sum_r \mu^a_{\alpha_r}v^{\alpha_r}$$
$$+4k^a_1\left(\lambda^2_a-1\right)e^{k^a_2\left(\lambda^2_a-1\right)^2}\sin^2\beta_a v^2$$

$$\sigma^a_{zz}(r)=-p^a(r)+\sum_r \mu^a_{\alpha_r}\lambda_z^{\alpha_r}$$
$$+4k^a_1\left(\lambda^2_a-1\right)e^{k^a_2\left(\lambda^2_a-1\right)^2}\cos^2\beta_a\lambda_z^2$$

Substituting stresses (21a), (21b) and (22) into Eq. (11a), Eq. (11b), integrating them $[a,R]$ with respect to r,

$$-p^m(r,t)+p^m(a,t)+\sum_r \mu^m_{\alpha_r}\lambda_z^{-\alpha_r}v^{-\alpha_r}+J^m(r)$$
$$=\rho\dot{a}^2\frac{a^2-r^2+2r^2\ln r-2r^2\ln a}{2r^2}+\rho a\ddot{a}(\ln r-\ln a) \tag{23a}$$

$$-p^a(r,t)+p^a(a,t)+\sum_r \mu^a_{\alpha_r}\lambda_z^{-\alpha_r}v^{-\alpha_r}+J^a(r)$$
$$=\rho\dot{a}^2\frac{a^2-r^2+2r^2\ln r-2r^2\ln a}{2r^2}+\rho a\ddot{a}(\ln r-\ln a) \tag{23b}$$

$$-p^m(r)+\sum_r \mu^m_{\alpha_r}\lambda_z^{-\alpha_r}v^{-\alpha_r}+p^m(a)+J^m(R)=0$$
$$-p^a(r)+\sum_r \mu^a_{\alpha_r}\lambda_z^{-\alpha_r}v^{-\alpha_r}+p^a(a)+J^a(R)=0$$

where,

$$J^m(R)=\frac{1}{\lambda_z v^2 R}\int_a^R\left[\sum_r \mu^m_{\alpha_r}\left(\lambda^{-\alpha_r}v^{-\alpha_r}-v^{\alpha_r}\right)\right.$$
$$\left.-4k^m_1\left(\lambda^2_m-1\right)e^{k^m_2\left(\lambda^2_m-1\right)^2}\sin^2\beta_m v^2\right]\mathrm{dR}$$

$$J^m(r)=\int_a^r\frac{1}{r}\left[\sum_r \mu^m_{\alpha_r}(\lambda_z^{-\alpha_r}v^{-\alpha_r}-v^{\alpha_r})\right.$$
$$\left.-4k^m_1\left(\lambda^2_m-1\right)e^{k^m_2\left(\lambda^2_m-1\right)^2}\sin^2\beta_m v^2\right]\mathrm{d}r$$

$$J^a(r)=\int_a^d\frac{1}{r}\left[\sum_r \mu^m_{\alpha_r}(\lambda_z^{-\alpha_r}v^{-\alpha_r}-v^{\alpha_r})\right.$$
$$\left.-4k^m_1\left(\lambda^2_m-1\right)e^{k^m_2\left(\lambda^2_m-1\right)^2}\sin^2\beta_m v^2\right]\mathrm{d}r$$
$$+\int_d^r\frac{1}{r}\left[\sum_r \mu^a_{\alpha_r}(\lambda_z^{-\alpha_r}v^{-\alpha_r}-v^{\alpha_r})\right.$$
$$\left.-4k^a_1\left(\lambda^2_a-1\right)e^{k^a_2\left(\lambda^2_m-1\right)^2}\sin^2\beta_a v^2\right]\mathrm{d}r$$

$$J^a(R)=\frac{1}{\lambda_z v^2 R}\int_a^d\left[\sum_r \mu^m_{\alpha_r}\left(\lambda^{-\alpha_r}v^{-\alpha_r}-v^{\alpha_r}\right)\right.$$
$$\left.-4k^m_1\left(\lambda^2_m-1\right)e^{k^m_2\left(\lambda^2_m-1\right)^2}\sin^2\beta_m v^2\right]\mathrm{dR}$$
$$+\frac{1}{\lambda_z v^2 R}\int_d^R\left[\sum_r \mu^a_{\alpha_r}\left(\lambda^{-\alpha_r}v^{-\alpha_r}-v^{\alpha_r}\right)\right.$$
$$\left.-4k^a_1\left(\lambda^2_a-1\right)e^{k^a_2\left(\lambda^2_{ma}-1\right)^2}\sin^2\beta_a v^2\right]\mathrm{dR}$$

$$d=r(D,t)=[\frac{1}{\lambda_z}(D^2-A^2)+a^2]^{\frac{1}{2}}$$

Substituting Eq. (23a) and Eq. (23b) into stresses (21a) and (21b) and using the continuity condition σ_{rr} (13),

$$p^m(a,t)=p^a(a,t)=p(a,t) \tag{24}$$

Using the boundary conditions (12), we have $p(a,t)=p(t)$ and

$$q=\left[\begin{array}{c}\sum_r \mu^m_{\alpha_r}\left(\lambda_z^{-\alpha_r-1}v^{-1-\alpha_r}-v^{\alpha_r-1}\lambda_z^{-1}\right)\\ \int_{v(a)}^{v(d)}\frac{-4k^m_1\left(\lambda^2_m-1\right)e^{k^m_2\left(\lambda^2_m-1\right)^2}\sin^2\beta_m\lambda_z^{-1}v}{\lambda_z^{-1}-v^2}\mathrm{d}v\end{array}\right]$$
$$+\left[\begin{array}{c}\sum_r \mu^a_{\alpha_r}\left(\lambda_z^{-\alpha_r-1}v^{-1-\alpha_r}-v^{\alpha_r-1}\lambda_z^{-1}\right)\\ \int_{v(d)}^{v(b)}\frac{-4k^a_1\left(\lambda^2_a-1\right)e^{k^a_2\left(\lambda^2_a-1\right)^2}\sin^2\beta_a\lambda_z^{-1}v}{\lambda_z^{-1}-v^2}\mathrm{d}v\end{array}\right] \tag{25}$$

$$p(t)=\rho\frac{a^2-b^2+2b^2\ln b-2b^2\ln a}{2b^2}\dot{a}^2 + \rho a\ddot{a}(\ln b-\ln a)-J^a(b)$$

With transformation Eq. (16), we have

$$\begin{aligned} p(t) &= \rho\tfrac{a^2-b^2+2b^2\ln b-2b^2\ln a}{2b^2}\dot{a}^2+\rho a\ddot{a}(\ln b-\ln a)\\ &-\int_{v(a)}^{v(d)}[\sum_r \mu_{\alpha_r}^m(\lambda_z^{-\alpha_r}v^{-\alpha_r}-v^{\alpha_r})\\ &-4k_1^m\left(\lambda_m^2-1\right)e^{k_2^m\left(\lambda_m^2-1\right)^2}\sin^2\beta_m v^2]\tfrac{v^{-1}dv}{1-\lambda_z v^2}\\ &-\int_{v(d)}^{v(b)}[\sum_r \mu_{\alpha_r}^a(\lambda_z^{-\alpha_r}v^{-\alpha_r}-v^{\alpha_r})\\ &-4k_1^a\left(\lambda_a^2-1\right)e^{k_2^a\left(\lambda_m^2-1\right)^2}\sin^2\beta_a v^2]\tfrac{v^{-1}dv}{1-\lambda_z v^2} \end{aligned} \tag{26}$$

$$v(b)=\left(\frac{1}{\lambda_z}\left(1-\frac{a^2}{b^2}\right)+\frac{r^2(a)}{b^2}\right)^{\frac{1}{2}},\ v(a)=\frac{r(a)}{a}$$

This second-order nonlinear ordinary differential equation provides an exact relationship between the inflation deformation and the applied pressure.

Let $\frac{a}{A}=x(t),\delta_1=\frac{B^2}{A^2}-1,\delta_2=\frac{D^2}{A^2}-1$

Then $\frac{b^2}{B^2}=\frac{\frac{1}{\lambda_z}\delta_1+x^2}{1+\delta_1},\frac{d^2}{D^2}=\frac{\frac{1}{\lambda_z}\delta_2+x^2}{1+\delta_2},\frac{b^2}{a^2}=1+\frac{\frac{1}{\lambda_z}\delta_1}{\lambda^2},\frac{d^2}{a^2}=1+\frac{\frac{1}{\lambda_z}\delta_2}{\lambda^2}$

Eq. (26) may be rewritten as

$$\begin{aligned} p(t) &= \rho A^2 x\ddot{x}\ln\sqrt{1+\frac{\lambda_z^{-1}\delta_1}{x^2}}\\ &+\rho A^2\dot{x}^2\left[\ln\sqrt{1+\frac{\lambda_z^{-1}\delta_1}{x^2}}-\frac{\lambda_z^{-1}\delta_1}{2(x^2+\lambda_z^{-1}\delta_1)}\right]\\ &-f(x,\delta_1,\delta_2) \end{aligned} \tag{27}$$

In which,

$$\begin{aligned} f(x,\delta_1,\delta_2) &= \int_x^{\sqrt{\frac{\lambda_z^{-1}\delta_2+x^2}{1+\delta_2}}}[\sum_r \mu_{\alpha_r}^m(\lambda_z^{-\alpha_r}v^{-\alpha_r}-v^{\alpha_r})\\ &-4k_1^m\left(\lambda_m^2-1\right)e^{k_2^m\left(\lambda_m^2-1\right)^2}\sin^2\beta_m v^2]\tfrac{v^{-1}dv}{1-\lambda_z v^2}\\ &+\int_{\sqrt{\frac{\lambda_z^{-1}\delta_2+x^2}{1+\delta_2}}}^{\sqrt{\frac{\lambda_z^{-1}\delta_1+x}{1+\delta_1}}}[\sum_r \mu_{\alpha_r}^a(\lambda_z^{-\alpha_r}v^{-\alpha_r}-v^{\alpha_r})\\ &-4k_1^a\left(\lambda_a^2-1\right)e^{k_2^a\left(\lambda_m^2-1\right)^2}\sin^2\beta_a v^2]\tfrac{v^{-1}dv}{1-\lambda_z v^2} \end{aligned}$$

The corresponding initial conditions are

$$x(0)=1,\dot{x}(0)=0 \tag{28}$$

Observing $V=\frac{dx}{dt},\frac{d^2x}{dt^2}=V\frac{dV}{dx}$ and integrating Eq. (27) with respect to x,

$$\begin{aligned} (x^2-1)p(t) &= x^2V^2\ln\sqrt{1+\frac{\lambda_z^{-1}\delta_1}{x^2}}\\ &-2\int_1^x xf(x,\delta_1,\delta_2)dx \end{aligned} \tag{29}$$

From the theory of vibrations, the motion $x(t)$ is periodic if and only if the $x\sim\dot{x}=V$ curve in the phase diagram is closed and owns a finite period $T=\oint\frac{dx}{V}$. For a given constant pressure p_0, the period motion $x(t)$ will occur if there is a root $x>0$ for Eq. (29) when $V=0$. Letting $V=0$ in Eq. (29) leads to

$$(x^2-1)p_0=-2\int_1^x xf(x,\delta_1,\delta_2)dx \tag{30}$$

For a given pressure p_0, if there is a root $x>0$ for Eq. (30), then it is the maximum radius of the internal surface of the tube in the oscillation process and denotes by $x_{\max}$. Thus the internal surface of the tube will expand until its radius reaches the maximum value $x_{\max}$, then it would contract and

repeat the cycle process.

$$\sigma_{rr}^m = -q- \left[\begin{array}{c} \sum\limits_r \mu_{\alpha_r}^m \left(\lambda_z^{-\alpha_r-1} v^{-1-\alpha_r} - v^{\alpha_r-1} \lambda_z^{-1} \right) \\ \int\limits_{v(a)}^{v(R)} \frac{-4k_1^m \left(\lambda_m^2 - 1 \right) e^{k_2^m \left(\lambda_m^2 - 1 \right)^2} \sin^2 \beta_m \lambda_z^{-1} v}{\lambda_z^{-1} - v^2} \mathrm{d}v \end{array} \right]$$

$$\sigma_{\theta\theta}^m = \sum_r \mu_{\alpha_r}^m \left(v^{\alpha_r} - \lambda_z^{-\alpha_r} v^{-\alpha_r} \right) + 4k_1^m \left(\lambda_m^2 - 1 \right) e^{k_2^m \left(\lambda_m^2 - 1 \right)^2} \sin^2 \beta_m v^2 + \sigma_{rr}^m$$

$$\sigma_{zz}^m = \sum_r \mu_{\alpha_r}^m \left(\lambda_z^{\alpha_r} - \lambda_z^{-\alpha_r} v^{-\alpha_r} \right) + 4k_1^m \left(\lambda_m^2 - 1 \right) e^{k_2^m \left(\lambda_m^2 - 1 \right)^2} \cos^2 \beta_m \lambda_z^2 + \sigma_{rr}^m$$

$$\sigma_{rr}^a = -q- \left[\begin{array}{c} \sum\limits_r \mu_{\alpha_r}^m \left(\lambda_z^{-\alpha_r-1} v^{-1-\alpha_r} - v^{\alpha_r-1} \lambda_z^{-1} \right) \\ \int\limits_{v(a)}^{v(d)} \frac{-4k_1^m \left(\lambda_m^2 - 1 \right) e^{k_2^m \left(\lambda_m^2 - 1 \right)^2} \sin^2 \beta_m \lambda_z^{-1} v}{\lambda_z^{-1} - v^2} \mathrm{d}v \end{array} \right] - \left[\begin{array}{c} \sum\limits_r \mu_{\alpha_r}^a \left(\lambda_z^{-\alpha_r-1} v^{-1-\alpha_r} - v^{\alpha_r-1} \lambda_z^{-1} \right) \\ \int\limits_{v(d)}^{v(R)} \frac{-4k_1^a \left(\lambda_a^2 - 1 \right) e^{k_2^a \left(\lambda_a^2 - 1 \right)^2} \sin^2 \beta_a \lambda_z^{-1} v}{\lambda_z^{-1} - v^2} \mathrm{d}v \end{array} \right]$$

$$\sigma_{\theta\theta}^a = \sum_r \mu_{\alpha_r}^a \left(v^{\alpha_r} - \lambda_z^{-\alpha_r} v^{-\alpha_r} \right) + 4k_1^a \left(\lambda_a^2 - 1 \right) e^{k_2^a \left(\lambda_a^2 - 1 \right)^2} \sin^2 \beta_a v^2 + \sigma_{rr}^a$$

$$\sigma_{zz}^a = \sum_r \mu_{\alpha_r}^a \left(\lambda_z^{\alpha_r} - \lambda_z^{-\alpha_r} v^{-\alpha_r} \right) + 4k_1^a \left(\lambda_a^2 - 1 \right) e^{k_2^a \left(\lambda_a^2 - 1 \right)^2} \cos^2 \beta_a \lambda_z^2 + \sigma_{rr}^a$$

5 Results

5.1 Results for the normal condition

Curves $x_{\max} \sim p_0$ for the arterial wall with different axial stretches from numerical computation of Eq. (30) are shown in Fig.3. Phase diagrams ($x \sim V$ curves) of the oscillation corresponding to different pressures from numerical computation of Eq. (29) are shown in Fig.4. The geometrical and material parameters as well as the loading conditions used in calculations are taken from Holzapfel et al. 2000, Holzapfel et al. 2002 and Driessen et al. 2003. Reference values are summarized in Table 1.

It is shown that the maximum value $x_{\max}$ for the motion of the internal surface of the arterial wall

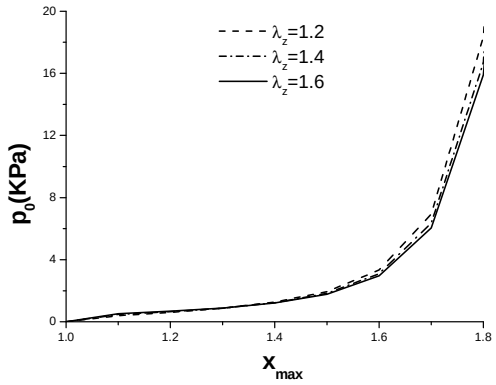

Figure 3: $x_{\max} \sim p_0$ curves

increases with the increasing of the pressure and the corresponding phase curves in the phase plane are closed curves which are symmetric about x-axis. Thus the arterial wall undergoes nonlinear periodic oscillation and no aneurysms are formed under a suddenly applied constant internal pressure in the case of the normal condition. The axial stretch of the deformation may effect on the deformation and stresses but it is not too large.

Expressions of (21a) and (21b) yield the distribution of stresses for the arterial wall. Distribution of stresses for the arterial wall under a given normal state ($\lambda_z = 1.6, p_0 = 15.5kPa, x_{\max} = 1.8$) is shown in Fig.5. The change of stresses at the inner surface with its deformation in the case of a normal state $\lambda_z = 1.6$ is shown in Fig. 6.

It is shown that all stresses for the media part of the arterial wall are larger than that for the adventitia part and the circumferential stress is much larger than the other stresses. The circumferential stress and the axial stress increase with the increasing of radius, and they are discontinuous with a jumping at the interface of the media and the adventitia. The radial stress is so little that it may be ignored. At the same time, all the stress components increase with the increasing of the inflation of the arterial wall and the circumferential stress increases most sharply. Results from this model are coincident with the clinical or experiment observations (Chyatte et al 1999, Humphrey

Table 1: Reference values of the parameters used in the model

Parameter	Description	Value
a	Inner radius (undeformed configuration)	0.71mm
d	Interface for the media and adventitia	0.97mm
b	Outer radius	1.1mm
μ_m	Shear modulus for the media	3.0kPa
μ_a	Shear modulus for the adventitia	0.3kPa
k_{1m}	Fiber parameter for the media	1.18 kPa
k_{1a}	Fiber parameter for the adventitia	0.28 kPa
k_{2m}	Fiber parameter for the media	0.84
k_{2a}	Fiber parameter for the adventitia	0.71
q	Internal pressure	13.0 kPa
	Axial stretch	1.6∼1.2
β_m	Initial fiber direction for the media	80^0
β_a	Initial fiber direction for the adventitia	50^0

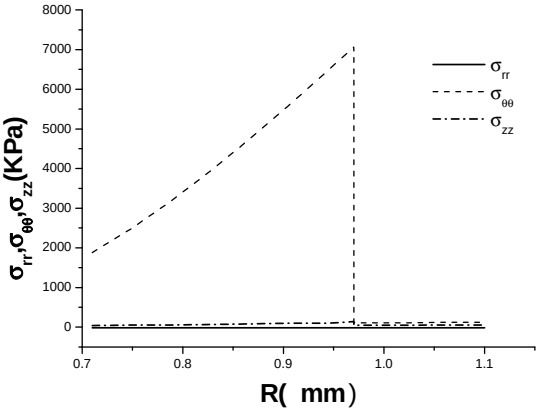

Figure 4: Stress distributions ($\lambda_z = 1.6, p_0 = 15.5kPa, x_{\max} = 1.8$)

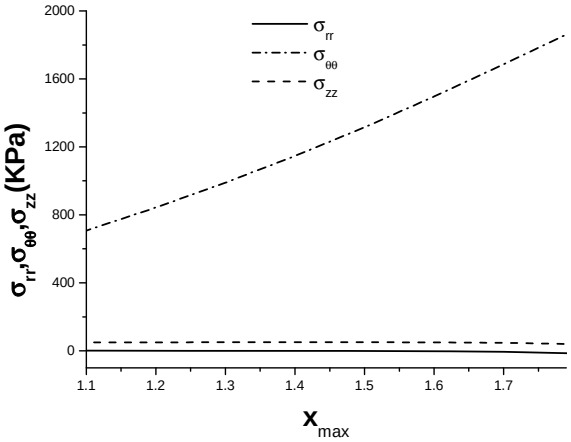

Figure 5: Change of stresses ($\lambda_z = 1.6$)

2003).

5.2 Results for abnormal conditions

To analyze the possibility of the formation of aneurysm, we need to consider situations of some abnormal conditions, such as the change of the shear modulus of the matrix and the change of the stiffness and the directions of the fibers. These changes may take place due to ages and vascular disease or disorders (Holzapfel and Ogden 2003, Humphrey 2003a). These effects may be reflected by different values of material parameters for the strain energy function of the arterial wall. Curves $x_{\max} \sim p_0$ and the phase diagrams for the arterial wall under abnormal conditions with certain material parameters from numerical computation of Eq. (30) and (29) are shown in Fig.7∼9. It is found that the decrease of the shear modulus of the matrix does not give rise to any obvious difference to the $x_{\max} \sim p_0$ curves. This is due to the fact that the fibers are much stiffer than the matrices and they bear the main part of the load.

The $x_{\max} \sim p_0$ curves and the phase diagrams change with the change of the stiffness or the directions of fibers. Typical $x_{\max} \sim p_0$ curve as shown in Fig.7 or Fig.9 shows typical insta-

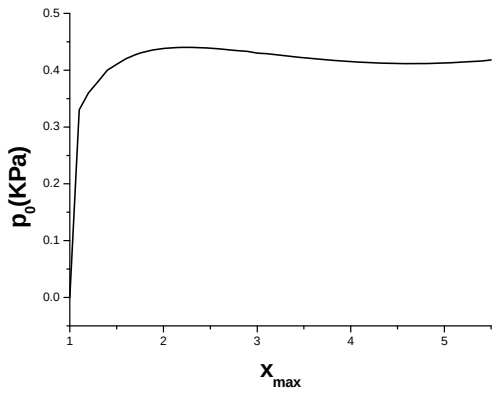

Figure 6: $x_{\max} \sim p_0$ curves ($\lambda_z = 1.6$,$k_{1m} = 0kPa, k_{1a} = 0kPa$)

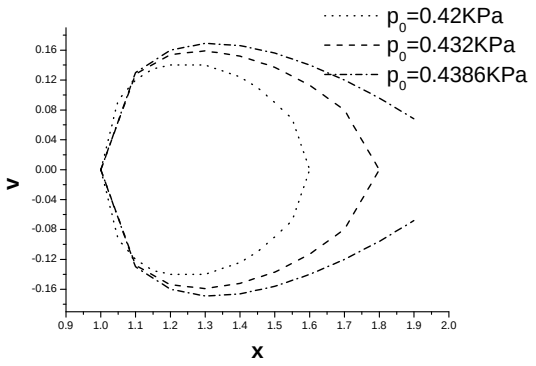

Figure 7: Phase diagram ($\lambda_z = 1.6$,$k_{1m} = 0kPa, k_{1a} = 0kPa$)

bility of nonlinear response for the arterial wall with highly reduced fiber stiffness or with collagen fibers orient toward the axial direction to a certain degree.

There generally exhibit a maximum $(x_{\max,1}, p_{0,1})$ and a minimum$(x_{\max,2}, p_{0,2})$ on the curves. When the pressure is less than the maximum value, the oscillation amplitude keeps increasing. However, when it reaches the maximum value, the oscillation amplitude will decrease with it. Finally, when it reaches the minimum value, the oscillation amplitude will increase with it again. At the same time, when the pressure is less than the maximum value, the phase curves are closed curves. Thus the arterial wall will take periodic oscillation. But

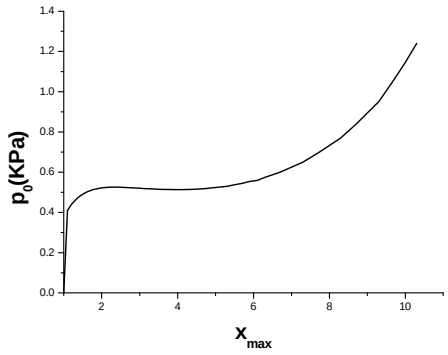

Figure 8: $x_{\max} \sim p_0$ curves ($\lambda_z = 1.6$,$\beta_m = 5^0, \beta_a = 5^0$)

when the pressure reaches the maximum value, the phase curves are not closed curves. Thus the curve between $(x_{\max,1}, p_{0,1})$ and $(x_{\max,2}, p_{0,2})$ is unstable and a large jump in deformation and stresses responses occur. An aneurysm is formed and it may get a quickly expanding following its formation. So the maximum pressure may be taken as the critical pressure for the formation of aneurysm. It is shown that the critical pressure decreases with the decreasing of the stiffness for the fibers or with the adjacent of the fibers to the axial direction.

It is widely thought that if the stress induced by pressure is less than the strength of the arterial wall, the aneurysm will keep its inflation state. But if this stress is larger than the strength of the arterial wall, the rupture will occur (Humphrey 2003b). Based on the observation of Humphrey (Humphrey 2003b), two human secular aneurysms exhibited critical breaking stresses on the order of $\sigma_c = 1 \sim 2MPa$, $\sigma_c = 1.6MPa$ is taken out to model the rupture of the aneurysm. The change of stresses at the inner surface with the increasing of deformation in two typical abnormal states $\beta_m = 5^0, \beta_a = 5^0$ and $k_{1m} = 0kPa, k_{1a} = 0kPa$ is shown in Fig. 10 and Fig.11.

It is shown in the figures 10$\sim$11 that the stress components increase with the increasing of pressure. The axial stress may reach $\sigma_c = 1.6MPa$ for

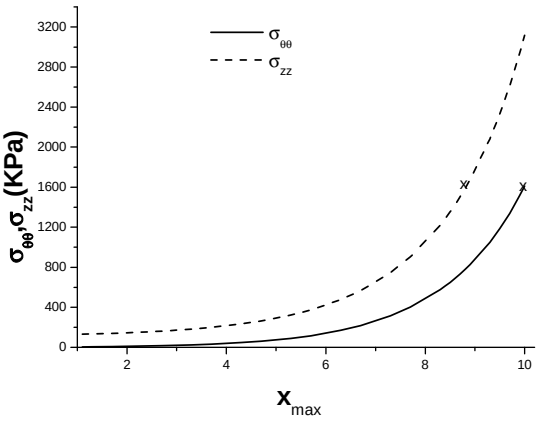

Figure 9: Change of stresses for aneurysm ($\lambda_z = 1.6$,$\beta_m = 5^0, \beta_a = 5^0$)

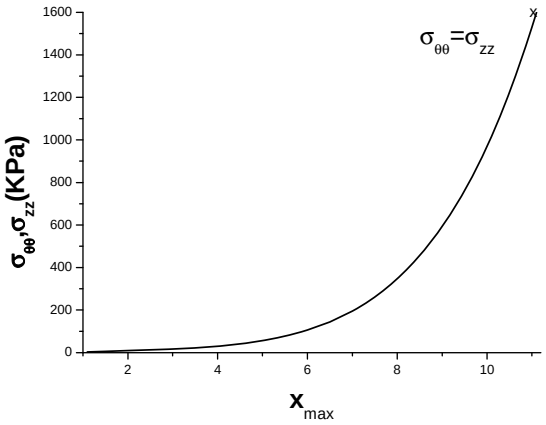

Figure 10: Change of stresses for aneurysm ($\lambda_z = 1.6$,$k_{1m} = 0kPa, k_{1a} = 0kPa$)

pressure$p_0 = 0.874KPa$ $(x_{\max} = 8.9)$ while the circumferential stress may reach $\sigma_c = 1.6MPa$ for pressure $p_0 = 1.143KPa(x_{\max} = 10.0)$ under the first state. The axial stress or the circumferential stress may reach $\sigma_c = 1.6MPa$ for pressure $p_0 = 0.879KPa$ $(x_{\max} = 11.1)$ under the second state. So the normal blood pressure $(13.0KPa)$ is large enough for the rupture of the aneurysm. Thus the aneurysm will expand rapidly to a certain extent as large as $x_{\max} = 11$ after its formation and will rupture at last. This procedure is agreement with the observation for intracranial saccular aneurysms described by Humphrey (Humphrey 2003b).

6 Discussions

The dynamical response along with the possibility of the formation and the rupture of an aneurysm for arterial wall with collagen fibers distributed in two preferred directions under a suddenly applied constant internal pressure may be described by the model presented in the paper. The arterial wall undergoes nonlinear periodic oscillation and no aneurysms are formed under the normal condition. However, the effect of collagen fibers distributed in the arterial wall is remarkable. Both of the stiffness and the distribution direction of the collagen fibers affect on the deformation and stress distribution of the arterial wall. They also affect on the formation and rupture of aneurysm. An aneurysm may be formed if the stiffness of the fibers is decreased to a certain degree or the direction of the fibers is orient towards the axial direction to a certain degree. These cases may be engendered by some risk factors such as hypertension, heavy alcohol consumption, cigarette smoking. The aneurysm may expand to much large extent after its formation. Finally, the aneurysm may rupture if the stress in the aneurysm is larger than the critical breaking stress. The normal blood pressure is large enough for the rupture of the aneurysm.

Compared to the corresponding static problem, it is easier to form an aneurysm under a suddenly applied constant pressure. For example, the critical pressure for the formation of aneurysm is $0.44KPa$ under a suddenly applied constant pressure in the case of $\lambda_z = 1.6$,$k_{1m} = 0kPa, k_{1a} = 0kPa$ in this paper, while it is $0.59KPa$ under the same static uniform pressure (Ren 2007). So the effect of dynamical response of the arterial on the formation and rupture of aneurysm can not be ignored.

Some dynamical responses along with the possibility of the formation and the rupture of an aneurysm have been described, but in fact the arterial wall experiences a periodic or nearly periodic internal pressure. Here is a need to understand well the formation and rupture of aneurysms under a periodic or nearly periodic internal pressure and our continued efforts will be directed to-

ward this.

Acknowledgement: This work was supported by the National Nature Science Foundation of China (10772104), the innovation project of Shanghai Municipal Education Commission (09YZ12) and Shanghai Leading Academic Discipline Project (S30106).

References

1. Chou-Wang M-S, Horgan C.O., 1989. Cavitation in nonlinear elastodynamic for neo-Hookean materials. Int. J. of Engng. Sci. 27, 967-973.

2. David, G., Humphrey J.D., 2003, Further evidence for the dynamic stability of intracranial saccular aneurysms. J. Biomech. 36, 1043-1150.

3. Driessen N.J.B., Peters, G. W. M., Huyghe, J.M., et. al., 2003. Remodeling of continuously distributed collagen fibers in soft connective tissues. J. Biomech. 36(8), 1111-1158.

4. Driessen N.J.B., Wilson W., Bouten C.V.C, et. al., 2004. A computational model for collagen fiber remodeling in the arterial wall. J of Theoretical Biology 226, 53-64.

5. Fung Y.C., 1990. Biomechanics: Motion, Flow, Stress and Growth. Springer-Verlag, New York.

6. Gasser T.C., Ogden R.W., Holzapfel G.A., 2006. Hyperelastic modeling of arterial layers with distributed collagen fiber orientations. J. R. Soc. Interface 3, 15-35.

7. Gent A.N., 2005. Elastic instability in rubber. Int. J. of Nonlinear Mechanics 40, 165-175.

8. Haslach A.D., Humphrey J.D., 2004. Dynamics of biological soft tissue and rubber: internally pressurized spherical membranes surrounded by a fluid. Int. J. of Nonlinear Mechanics 39, 399-420.

9. Haughton D.M., Ogden R.W., 1978. On the incremental equations in non-linear elasticity-II: Bifurcation of pressurized spherical shells. J. Mech. Phys. Solids 26, 111-138.

10. He C.M., Roach M., 1993. The composition and mechanical properties of abdominal aortic aneurysms. J Vasc. Surg. 20, 6-13.

11. Holzapfel G.A., Weizalker H.W., 1998. Biomechanical behavior of the arterial wall and its numerical characterization. Comput. Bio. Med. 28, 377-393.

12. Holzapfel G.A., Gasser T.C., Ogden R.W., 2000. A new constitutive framework for arterial wall mechanics and a comparative study of material models. J. of Elasticity 61, 1-48

13. Holzapfel G.A., Gasser T.C., Stadler M., 2002. Structural model for the viscoelastic behavior of arterial walls, continuum formulations and finite element analysis. Eur. J. Mech. A/Solids 21(3), 441-463.

14. Holzapfel G.A., Ogden R.W., 2003. Biomechanics of soft tissue in cardiorascular systems. Wien Springer. CISM courses and lectures, 441.

15. Holzapfel G.A., Sommer G., Regitnig P., 2004. Anisotropic mechanical properties of tissue components in human atherosclerotic plaques. J. Biomech. Eng. 126, 657-665.

16. Humphrey J.D., 1998. Computer methods in membrane biomechanics. Comp. Meth. Biomech. Biomed., Eng. 1, 171-210.

17. Humphrey J.D., 1999. Remodeling of a collagenous tissue at fixed lengths. J. Biomech. Eng. 121(6), 591-597.

18. Humphrey J.D., Canham P.B., 2000. Structure, mechanical properties and mechanics of intracranial saccular aneurysms. J. of Elasticity 61, 49-81.

19. Humphrey J.D., 2002. Cardiovascular solid Mechanics. Cells, Tissures and Organs. Springer –Verlag NewYork, New York.

20. Humphrey J.D., 2003a. Intracranial saccular aneurysms. In: Holzapfel G.A., Ogden R.W. (ed.), Biomechanics of soft tissue in cardiovascular systems. Springer WienNewYork, New York, 185-220.

21. Humphrey J.D., 2003b. Continuum biomechanics of soft biological tissues. Proc. R. Soc. A. 459, 1-44.

22. Kroon M., Holzapfel G.A., 2008, Estimation of the distributions of anisotropic, elastic properties and wall stresses of saccular cerebral aneurysms by inverse analysis. Proceedings of the Royal Society A, 464, 807-825.

23. Lanne T., Sonesion B., Bergquist D.,1992. Diameter and compliance in the male human abdominal aorta: influence of age and aortic aneurysm. Eur. J Vasc. Surg. 6, 178-189.

24. Neren R. M., Selihtar D., 2001. Vascular tissue engineering. Annu. Rev. Biomech. Eng. 3, 225-243.

25. Ogden R.W., 2002. Pseudo-elasticity and stress softening. In: Fu Y.B., Ogden R.W.(ed.), Nonlinear Elasticity. Cambridge University Press. Cambridge, 491-522.

26. Ogden R.W., 2003. Nonlinear elasticity, anisotropy, material stability and residual stresses in soft tissue. In: Holzapfel G.A., Ogden R.W.(ed.), Biomechanics of soft tissue in cardiovascular systems. Springer WienNewYork. New York, 65-108.

27. Olsen L., Maini P.K., Sherratt J.A., et. al., 1999. Mathematical modeling of anisotropy fibrous connective tissue. Math. Biosci. 15892), 145-170.

28. Papahariluon Y., 2006. A decoupled fluid structure approach for estimating wall stress in abdominal aortic aneurysms. J. Biomech. 39, 1111-1158.

29. Peng Y.H., Li X.Y., Wu S.G., 1999. A data-processing technique for the 3D static nonlinear mechanical properties of arterial wall. J. of Experiment Mechanics (in Chinese). 14, 425-431.

30. Ren Jiu-sheng, 2007. Inflation of an artery leading to aneurysm formation and rupture. Molecular and Cellular Biomechanics 4(1), 55-66

31. Shah A.D., Humphrey J.D., 1999. Finite strain elastodynamics of intracranial aneurysms. J. Biomech. 32, 593-595.

32. Vito R.P., Dixon S.A., 2003, Blood vessel constitutive models-1995-2002. Annu. Rev. Biomed. Eng., 5, 413-439.

33. Volokh K.Y., Vorp D.A., 2008, A model of growth and rupture of abdominal aortic aneurysm. J. Biomech, 41, 1015-1021.

34. Vorp D.A. 2007, Biomechanics of abdominal aortic aneurysm. J. Biomech. 40, 1887-1902.

35. Watton P.N., Hill N.A., Heil M., 2004. A mathematical model for the growth of abdominal aortic aneurysm. Biomechan Model Mechanobiol 3, 98-113.

36. Wilmink W.B.M., Quick C.R.G., Hubbard C.S., Dag N.E., 1999. The influence of screening on the incidence of ruptured abdominal aortic aneurysms. J Vasc. Surg. 30, 203-208.